International Journal of Impact Engineering 189 (2024) 104931

Contents lists available at ScienceDirect

International Journal of Impact Engineering

journal homepage: www.elsevier.com/locate/ijimpeng

Enhanced cross laminated timber (ECLT) for ballistic resistant design

Juliet Swinea [a], Kathryn Sanborn [a], Mark Weaver [b], Marco Lo Ricco [c], C.Adam Senalik [c], Lauren K. Stewart [a,*]

[a] Department of Civil and Environmental Engineering, Georgia Institute of Technology, Atlanta, GA, USA
[b] Karagozian & Case, Inc., USA
[c] USDA Forest Products Laboratory, USA

ARTICLE INFO

Keywords:
Cross-laminated timber (clt)
Enhanced or reinforced clt (eclt)
Ballistics

ABSTRACT

Cross-laminated timber (CLT), an engineered wood product, has grown in popularity in the United States over the last decade due to its ease of assembly, aesthetic appeal, and potential to serve as a sustainable and renewable alternative building material. The improved robustness of CLT over light-frame timber structures has increased its potential in force-protected infrastructure that must resist blast waves and ballistic projectile penetration, but softwood CLT is typically not sufficient to fulfill standard criteria for ballistic threats. To address these threats, enhanced CLT (ECLT) composite panels were manufactured with layers of various reinforcing materials (e.g., steel, FRP) placed between wood laminations. These panels were tested against various ballistic threats during two sets of laboratory tests in order to provide a basis for future research. The first set of testing subjected laboratory-produced Southern Yellow Pine (SYP) ECLT to 84 shots of 0.50-inch (1.27 cm) steel sphere projectiles to evaluate the performance of various reinforcing materials, layups, and fastening methods. A subsequent set of tests subjected commercially produced ECLT of steel-reinforced Spruce-Pine-Fir (South) (SPF-S) to 36 shots of NATO ammunition projectiles traveling at realistic, standard striking velocities. Except for a panel using four layers of a thin and finely woven steel hardware cloth, steel reinforcement was effective in stopping projectiles from all three types of NATO ammunition fired. Ultimately considering the results of these two sets of tests, an initial cost-benefit structure was developed and discussed to compare ECLT configurations holistically, a multi-material wood analytical model framework was established and compared to experimental results, and the first ballistic experimental database for ECLT was created.

1. Introduction

Infrastructure designed for the U.S. Department of State (DOS) and U.S. Department of Defense (DOD) often must meet blast, ballistic, and forced entry requirements to address heightened threats of warfare, terrorism, violent protests, or criminal activity. Historically, DOS and DOD infrastructure exposed to these threats have been constructed with concrete, masonry, and steel [1]. In recent years, cross-laminated timber (CLT) panels have emerged as an engineered wood product of size comparable to precast concrete panels. The lightweight and sustainability of CLT, made from abundant stock sizes of renewable softwood lumber, has made wood structures capable of longer spans and taller building heights. In addition to being a versatile building material for structures of commercial and institutional scale, the robustness of CLT has been developed and studied as a structural building material for use in force protection applications, where wood had previously been displaced by more ductile steel and reinforced concrete materials [1–7].

1.1. Cross laminated timber (CLT)

Most commonly, standard CLT is formed from stacked, solid sawn lumber boards cut with various thicknesses and widths. It is composed of multiple wood lamina to create panels that are generally between three and nine inches thick [8]. Due to wood's orthotropic material properties, adjacent lamina are typically oriented perpendicularly to maximize each component's individual strength. The weakness of each wood member, oriented along the tangential axis is minimized, producing a composite material with high strength and stiffness [9]. Due to the layered and composite nature of CLT, panels are highly customizable if modifications are coordinated during manufacture. In-situ modifications are also possible to some extent, though CLT construction, similar to precast concrete and in contrast to light-frame timber, mostly involves

* Corresponding author.
E-mail address: lauren.stewart@ce.gatech.edu (L.K. Stewart).

https://doi.org/10.1016/j.ijimpeng.2024.104931
Received 29 August 2023; Received in revised form 14 February 2024; Accepted 27 February 2024
Available online 14 March 2024

prefabrication.

1.2. CLT in force protection

Since the latter half of the twentieth century, wood has not typically been considered in the design of protective structures, and therefore a limited number of experiments have been performed assessing wood construction against blast and ballistic threats. This is due to the discrepancy in strength as compared to other materials and the impracticality of efficiently and economically resisting DOS and DOD threats with light-frame wood construction [1,3]. However, CLT can achieve strengths greater than traditional wood elements and has advantages over the most prevalent protective materials, concrete and steel [3]. Over the past decade, efforts involving CLT panels and simulated (i.e., using shock tube) or actual blast loads have been led by the United States Army Corps of Engineers (USACE) Protective Design Center (PDC), the University of Ottawa, and WoodWorks. Three, five, and seven-ply CLT panels manufactured by Nordic Structures, DR Johnson, and SmartLam have been tested focused on flatwise bending response in the elastic and plastic regimes, response at the CLT boundary connections, and flatwise bending response of CLT panels retrofitted with either steel straps or glass fiber reinforced polymer (GFRP) sheets [10–14]. The results of two phases of high explosive field testing conducted by WoodWorks informed analysis guidance for CLT construction exposed to blast loads documented in PDC-TR 18–02 [5].

With the inherent benefits of lower weight and higher thermal efficiency, CLT is viable as a protective material. However, the limiting design constraint and driver of increased panel thicknesses is the need for ballistic resistance, as the thickness of CLT needed to resist small arms design threats is large and prohibitive [1–3]. For CLT to be realistically integrated into force protection applications, the system must be augmented to achieve realistic thicknesses. The laminated nature of CLT panels yields opportunities for introducing other non-wood materials into the composite, which would decrease the thickness of panel required to resist the ballistic threats required by DOS and DOD design standards. Multi-layer composite systems are an especially popular concept in ballistic-resistance soft and hard armor design incorporating metallic alloys, fibers, and combinations of the two [15–17]. For force protection applications, highly customizable armoring systems are required for situational decision making. For CLT as a building material, this customizability could involve the inclusion of enhancing layers that are integrated between the plies of the wood system.

1.3. Enhancing materials

Several different enhancing materials were selected based on their known properties that improved ballistic resistance. Some modifying layers were chosen based on their strengths and hardness, which either prevent perforation or slow projectile movement enough to prevent complete penetration. Other layers were chosen based on their ability to conform to the projectile and dissipate its energy enough across the panel's cross-sectional area to resist penetration. The enhancing layer materials were grouped as steels and fiber reinforced polymer (FRP) composites.

1.3.1. Steel

Steel as a protective material has been well studied under ballistic threats, and is historically prevalent in protective design specifications [18]. Five variations of commercially available steel plates were investigated as enhancing layers in this research, and a brief overview of each type is discussed here.

Mild steel is a popular building material due to its ductility but is typically not used in modern armor due to its lower strength and hardness relative to steel alloys with greater carbon contents and chemical additives. A previous study that included mild steel plates observed complete perforation when impacted by ogive-shaped armor-piercing projectiles. Thicker mild steel targets, up to almost 1-inch (2.54 cm), yielded similar results with slower residual velocities, and increased petal height on the front face [19]. However, this enhancing layer was chosen to investigate if its ductility, combined with the strength of the CLT sections, could dissipate the projectile's energy without failing.

Perforated metal plates have been shown to resist multiple threats with minimum loss of performance compared to solid metal plates, while significantly reducing weight due to perforations. The perforations, furthermore, may allow adhesives to penetrate and improve bonding contact of dissimilar materials. The staggered and slotted holes in the plate redirect projectiles upon impact, thus absorbing a significant amount of its energy. In this research, the holes were also oriented at an angle, which limits deflection and pass-through shots [20].

Expanded metal is manufactured differently than perforated metal and is typically a carbon steel sheet that has been slit and stretched into a rigid mesh with diamond shaped openings. Expanded metal is comprised of strands of metal with intersections called bonds, which form a sharp angle from the original flat sheet of metal and can divert a projectile's trajectory. Like perforated steel plates, expanded metal plates have a favorable strength-to-weight ratio and can either divert a projectile's trajectory or stop it at the plate after impact.

Steel mesh is a metallic fabric where intersecting steel wires are joined together by either welding or weaving. Steel mesh can be made in any shape and size with no metal waste produced after fabrication. Compared to a traditional metal sheet of the same size, steel mesh is lightweight, provides visibility and allows for airflow. In terms of force protection applications, steel wire mesh has been utilized in screen doors and window grilles to protect against intrusion and impact from debris [21].

High-hard steel is known for its high strength and is commonly used as applique armor for hardening vehicles [22]. Compared to mild steel, it is less ductile and has significantly greater hardness. In armor applications, it is typically heat treated to achieve even greater resistance to ballistic penetration. Although its weight and cost would make mass use in building construction unfeasible, this enhancing layer was chosen to explore the ease of ECLT production using this material and the possible delaminating effects of ballistic impact on the wood-steel interface.

1.3.2. Fiber reinforced composites (FRP)

Fiber reinforced polymer (FRP) composites offer high strength-to-weight ratios, and have been utilized as building and personal armor [18]. Three different FRP composites were investigated as enhancing layers in this research.

Aramid epoxy is a rigid board composed of layers of woven aramid fibers with a polyvinyl butyral (PVB) phenolic resin. This material was considered because the fibers have a high strength-to-weight ratio, high structural rigidity, and good resistance to abrasion and cutting.

Ultra-high molecular weight polyethylene (UHMWPE) is a fiber-based, low-weight composite laminate with four unidirectional sheets cross plied and held together with a polyurethane-based matrix. While the exact production details are proprietary, the general process involves the fiber manufacture in a high temperature gel-spinning process and then coated in resin, stacked crosswise to the desired thickness, and hot pressed [23].

Woven roving fiberglass fabric is a low-cost, high-strength material that is impact resistant. Much like aramid fabric, woven roving is composed of bundled threads oriented in two orthogonal directions with a basket-style weave. Once constructed, it has high tensile strength, is lightweight, and is compatible with epoxy bonding. Ballistic panels are commonly made with woven roving to absorb impact as well as trap shrapnel and spall in the plies. The material is often combined with other materials including foam core and concrete to form composite panels. Hybrid products using both carbon and glass fibers have also been the subject of ballistic impact studies.

The eight enhancing materials were selected due to the abundance of research in applications as ballistic resistant armoring systems, off the shelf commercial availability, and uniform sheet configuration for integration between wood layers. There is no previous experimental testing on ECLT, so a proof-of-concept program was performed to investigate the feasibility of manufacturing ECLT with the selected enhancing materials, as well as evaluate ballistic resistance including analysis of physical failure mechanisms between wood and enhancing material layers.

1.4. Research objectives

This paper summarizes the results from two separate ballistic experimental programs utilizing Southern Yellow Pine (SYP) and Spruce-Pine-Fir (South) (SPF-S) CLT panels [1,3]. Here, enhanced CLT (ECLT) is investigated and is distinct in that it introduces a layer of ballistic resistant material as compared to a hybrid layup which alternates various wood species [24–27].

Although both programs assessed the ballistic performance of ECLT, motivations differed, leading to different projectile, threat, and panel manufacturing choices. The research goals of both programs are defined below.

1.4.1. SYP eclt

The first publicly available partial and full penetration SYP CLT database used 0.50-inch (1.27 cm) steel sphere projectiles, and the same projectile was used in this study [2]. The research goals were to 1) Determine the most promising candidates and methodologies for fabricating ECLT, 2) Investigate the impacts of enhancing material distribution for ballistic resistance using energy analyses, 3) Scope and discuss a cost-benefit analysis for future decision makers, and 4) Develop and discuss an analytical multi-material model framework including wood.

1.4.2. SPF-S eclt

There is extremely limited publicly available ogive shaped ballistic data for CLT, so the results from this program will be used to draw broad initial conclusions, with the intent to conduct more experiments in the future. The research goal was to determine if a commercially fabricated ECLT panel, custom produced by SmartLam North America, with a max thickness of 10-inches (25.4 cm) could stop NATO rounds at realistic muzzle velocities.

2. Experiment description

The SYP ECLT panels were manufactured at the Georgia Institute of Technology's Digital Fabrication Laboratory and transported for ballistic testing at the US Army Corps of Engineer's Engineer Research and Development Center (ERDC) [3]. The SPF-S ECLT panels were manufactured by SMARTLAM and transported for ballistic testing at H.P. White Laboratory in Maryland [1].

3. Production methodology

3.1. SYP eclt production

Eight variations of ECLT were made using 5-ply SYP sawn lumber in accordance with guidelines and standards of the CLT Handbook: US Edition and Standards for Performance-Rated Cross-Laminated Timber ANSI/APA PRG 320–2012 (PRG 320) [3,29]. The impact cross-section of each specimen was sized to 12-inch width by 12-inch length (30.5 cm by 30.5 cm), with most enhancing layers placed between the second and third wood lamina to reduce the impact on the wood sub-components' other properties such as strength and stiffness. A key component of ECLT is the bond strength between the enhancing layer and the wood layers, which will be discussed below.

3.2. SPF-S eclt production

While the ECLT utilizing SYP were fabricated as 5-ply layups with enhancing layers positioned to limit impact on subcomponent properties, a series of 7-ply ECLT layups utilizing SmartLam SPF-S with enhancing layers positioned to produce a symmetric layup allowing equal inbound and rebound stiffness against blast threats were tested against NATO ballistic threats. To keep the ECLT panel designs to roughly 10-inches (25.4 cm) thick, a 7-ply SL-V4 panel manufactured by SmartLam was chosen with four types of enhancing layers incorporated. These CLT configuration were sized to 18-inch width by 18-inch length (45.7 cm by 45.7 cm) by nearly 10-inch thick (25.4 cm), and was manufactured using No. 2 SPF-S lumber in both directions.

3.2.1. Bond line integrity

A primary concern with embedding enhancing materials within a CLT panel is a bond line failure at ply interfaces. To counteract this, during the fabrication of the SYP ECLT specimens, enhancing material plates were either (1) mechanically affixed to the 2-ply and 3-ply sections using washer hex drive screws with 3/16-inch (0.47 cm) diameter and 6-inch (15.24 cm) length or (2) adhered to the two CLT sections using a two-part, resin and hardener, epoxy system with enhancing material sanded or media blasted to provide an effective adhering surface for the epoxy [3].

Additionally, for the SPF-S ECLT specimens, destructive testing involving a crowbar and 10-pound hammer was used to try and separate the embedded steel items from the adjacent timber plies. It was observed that the failure mode at the bond line was predominantly wood fiber tear, which indicated that the bond between the steel and the wood was not the weak point. This method is mainly valid for static analysis as the dynamic mechanisms of failure at the bond line depends on load rate and fracture area, but was performed to initially investigate the multi-material bond line manufacturing. Also, a cyclic delamination test in accordance with AITC Test T110 was performed to assess if the embedded steel plate designs would fail at the bond line. The results of this test indicated that although there were localized areas of delamination, no complete failures occurred. Fig. 1 shows the results post destructive testing [1].

4. Specimen

Twelve unique ECLT panels were configured with eight enhancing materials embedded between various plies within the CLT layups. The enhancing layer materials and configuration types used can be found in Table 1, and selected panels containing both SYP and SPF-S are shown in Fig. 2.

5. Experiment

5.1. SYP eclt experimental setup

Ballistic experiments were conducted at the US Army Corps of Engineers' Engineer Research and Development Center (ERDC). The experimental test set-up at ERDC consisted of an indoor, conditioned, ballistic range with a table-mounted smooth bore powder gun with 50-caliber barrel firing 0.50-inch (1.27 cm) spherical projectiles. Fig. 3 shows the firing apparatus. Four infrared photoelectric velocity screens were connected to two chronographs to capture two different velocity measurements as the projectile moved toward the target. The data from the screens was used to determine the striking velocity (v_s) based on the measured velocities and known distances between each of the screens and between the final screen and target. The ECLT specimens were secured to a floor mounted steel frame using ratchet straps, which enabled the specimens to be repositioned easily [3].

Two types of ballistic data were gathered depending on the effect of the shot. If the projectile perforated the CLT specimen, then a residual

Fig. 1. Post-test photographs of testing performed to assess bond line integrity (a) Destructive testing on Type 6: Embedded steel plate (thick) (b) AITC Test T110 on Type 6: Embedded steel plate (thick).

Table 1
Enhancing layer materials.

Enhancing Layer Material		Wood Species	Enhancing Layer Thickness in. (cm)	Specimen	Shots
Type 1	P900 Perforated Steel Plate	SYP	0.50 (1.27)	1	7
Type 2	Expanded Metal Plate	SYP	0.50 (1.27)	1	8
Type 3	Aramid Epoxy Panel	SYP	0.56 (1.42)	3	21
Type 4	Mild Steel Plate (1 layer)	SYP	0.25 (0.63)	2	10
Type 5	Mild Steel Plate (Thin, 2 layers)	SPF-S	0.24 (0.61)	3	9
Type 6	Mild Steel Plate (Thick, 2 layers)	SPF-S	0.50 (1.27)	3	9
Type 7	Steel Mesh (Fine, 4 layers)	SPF-S	0.504 (1.28)	3	9
Type 8	Steel Mesh (Coarse, 2 layers)	SPF-S	0.48 (1.22)	3	9
Type 9	High-Hard Steel Plate	SYP	0.25 (0.63)	2	10
Type 10	Ultra-High Molecular Weight Polyethylene (UHMWPE)	SYP	1.00 (2.54)	1	8
Type 11	Fiberglass Fabric (4-ply consolidated)	SYP	0.12 (0.31)	2	10
Type 12	Fiberglass Fabric (4-ply separated)	SYP	0.12 (0.31)	2	10

velocity was recorded based on the high-speed video capturing the round exiting the back face of the specimen. If the shot yielded only partial penetration and the projectile remained embedded in the specimen, then the depth of penetration was recorded. Ballistics testing is inherently variable as even factory-produced munitions shoot at a range of velocities, thus the goal with these experiments was to shoot multiple shots at the same approximate striking velocity across all specimen for comparison [3].

5.2. SPF-S eclt experimental setup

Ballistic experiments were conducted at HP White Laboratories in Aberdeen, Maryland. All testing was conducted on an indoor range at ambient conditions, in accordance with the general provisions of SD-STD.01.01 [28]. Testing was conducted using caliber 7.62 mm Ball, M80, 149 gr.; 5.56 mm Ball, M193, 55 gr.; 5.54 × 45 mm, and M855, 62 gr. ammunition. The test sample(s) were positioned 20 feet (6.1 m) from the muzzle of the barrel to produce zero-degree obliquity impacts. Photoelectric infrared screens were located at 5 feet (1.52 m) and 15 feet (4.57 m) which, in conjunction with electronic chronographs, were used to compute projectile velocities at 10 feet (3 m) forward of the muzzle. The striking velocity was computed using standard drag formulas. Complete and partial penetrations were determined by visual examination of the high-speed video to obtain the residual velocity of the complete penetrations. ECLT panel configurations were mounted on a rigid steel frame during the ballistic testing. Fig. 4 shows the ballistic setup for SPF-S ECLT [1].

The three projectiles from SD-STD-01.01, Revision G, were shot at the four ECLT panel configurations at the maximum velocities identified in Table 2 [18]. Each tile was shot with each type of SD-STD-01.01 projectile in a triangle pattern. Three duplicate tests were performed for each projectile/configuration panel combination leading to a total of 36 shots performed. The target velocities correspond to the upper bound velocity specified for each projectile in Table 3 of SD-STD-01.01, Revision G [18]. Residual velocities were measured using two high speed video feeds (i.e., from above and from the side) and penetration depth into the panel was measured using computed radiography.

6. Experimental results and analysis

All specimen, excluding those with the fiberglass fabric in the SYP CLT and fine embedded steel mesh in the SPF-S experienced only partial penetration. Therefore, the impacts of enhancing layers on the ballistic performance of CLT is significant as similar striking velocities that impact SYP and SPF-S CLT always result in perforation. In this section, experimental results will be presented with an initial ballistic resistance comparison between similar enhancing materials and wood species.

6.1. SYP

6.1.1. Perforated and expanded steel (Types 1 and 2)

CLT panels enhanced with P900 perforated (Type 1) and expanded (Type 2) steel plates were tested with target striking velocities of 2500 ft/s (762 m/s) resulting in average penetration depths of 3.42 inches (8.69 cm) and 3.61 inches (9.17 cm) respectively. There were no complete perforations, and penetrations past the enhancing materials reached a max at the front of the fourth ply, indicating that the enhancing layer dissipated enough of the projectile's energy to allow only shallow penetration. Shots close to the steel plate perforations resulted in deeper penetrations, demonstrating that the locations of perforation influenced the penetration depth. For the expanded metal panels, projectiles that impacted a bond were more effective than those that hit a single strand, and all fractured metal was contained within the CLT panel, minimizing shrapnel concerns.

Since both the perforated and expanded metal plates were 0.50 inches (1.27 cm) in thickness, and were embedded in the same location within the CLT layup, the raw penetration results can be directly compared. In Fig. 5, the vertical lines define the ply interface locations, and the grey area represents the enhancing layer. When the projectile

Fig. 2. Example panel configurations. (a) Type 2: Expanded Metal Plate (b) Type 5: Mild Steel Plate (Thin, 2 layers) (c) Type 6: Mild Steel Plate (Thick, 2 layers) (d) Type 7: Steel Mesh (Fine, 4 layers) (e) Type 8: Steel Mesh (Coarse, 2 layers) (f) Type 10: UHMWPE (g) Type 11: Fiberglass Fabric (4-ply consolidated) (h) Type 12: Fiberglass Fabric (4-ply separated).

perforated the expanded metal enhancing layer, the projectile penetrated further compared to the perforated metal enhancing layer showing the perforated metal was more effective in dissipating the projectile's energy when passed through the enhancing layer. This can be attributed to the different energy absorbing mechanisms, where the perforated metal holes were widened by the projectile, and the expanded metal fractured, with metal shrapnel loose and imbedded in the wood (Fig. 5). Although more shots perforated the expanded metal enhancing layer, the average penetration depth through the entire specimen was lower.

6.1.2. *Mild and hard steel (Types 4 and 9)*

CLT panels enhanced with mild (Type 4) and hard (Type 9) steel plates were tested with target striking velocities of 2500 ft/s (762 m/s) resulting in average penetration depths of 2.79 inches (7.08 cm) and 2.53 inches (6.4262 cm) respectively, indicating that the projectiles penetrated through the front CLT section but were stopped entirely by the steel plates. See Fig. 6 for a graphical representation of the penetration distribution for both enhancing materials.

The adhesion of the solid steel plates to the wood was a concern due to the natural curvature of the wood surface, and interfacial gaps resulting from fabrication were expanded by budging of the projectile on the rear side of the mild steel plate due to its ductility. Following the initial shot, small fractures developed in the wood and grew after successive shots toward the outer edges of the front and back sides of the steel interface. Although there was no evidence of complete delamination between the steel and wood, this cracking indicated the presence of high stresses in the interface between the two materials, likely the result of gaps formed by the inconsistent adhesion (Fig. 7).

Instead of bulging like the mild steel plate, the high-hard steel failed by plugging, indicated by holes in the steel plate and cylindrical slugs embedded in the rear CLT section beyond the enhancing layer. Damage to the projectiles indicated yielding against the harder steel plate (Fig. 7), and rebound of some shots off the high-hard steel plate resulted in projectiles captured in the front two plies of the panel. Unlike the ECLT enhanced with mild steel plate, fractures developed in the wood after the third or fourth shots and propagated toward the outer edges of the front and back sides of the steel interface with successive shots. This difference is likely due to the greater stiffness of high-hard steel, which results in less movement in response to ballistic impact. Similar to the

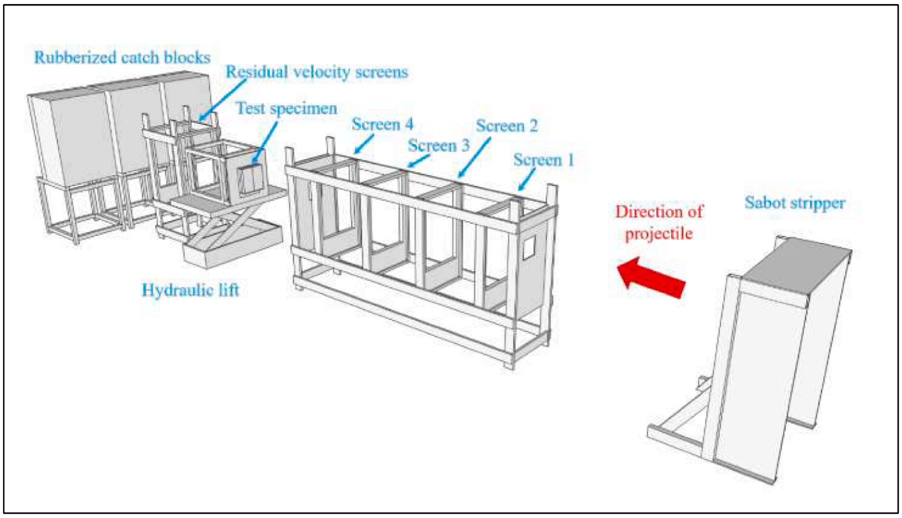

Fig. 3. Setup for ballistic experiments at the US Army Engineer Research and Development Center [9].

Fig. 4. Test Specimen Mounting for Ballistic Testing [1].

Table 2
SD-STD-01.01 (Revision G) Ballistic Resistance Test Ammunition.

Cartridge	Velocity Range ft/s (m/s)	
7.62 mm, M80, ball, 147 gr.	2700 (823)	2800 (853)
5.56 mm, M193, ball, 55 gr.	3135 (956)	3235 (986)
5.56 mm, M855, ball 63 gr.	2950 (899)	3050 (930)

mild steel plate configuration, the fractures indicated high stresses in the interface between the two materials. While less fracture in the wood was observed, this phenomenon creates concern on the best fabrication practices of this type of ECLT.

6.1.3. Aramid (Type 3)

Three panels enhanced with aramid epoxy were tested for a total of 21 shots. The target striking velocity of two of the panels was 2500 ft/s (762 m/s), resulting in no perforations and an average penetration depth of 4.55 in (11.56 cm). Below a striking velocity of 2600 ft/s (792.48 m/s), the projectiles were stopped in the first ply off the rear CLT section just beyond the enhancing layer, and at 2600 ft/s (792.48 m/s), the projectiles stopped in the back of the second ply off the enhancing layer.

To determine the limiting striking velocity, the third specimen was subjected to higher striking velocities. Six shots were taken with a minimum striking velocity of 2851 ft/s (869 m/s) and a maximum of 3041 ft/s (927 m/s). The three fastest shots achieved complete perforation, while the three slower shots partially penetrated, reaching the last wood ply of the panel. A graphical representation of penetration depths in the panel can be found in Fig. 8.

Using a conservation of energy approach, the difference in kinetic energy between the striking and residual velocities of the projectile was taken as the energy absorbing capacity of the material. Using baseline five ply SYP CLT striking and residual velocity data, the average energy absorbing capacity was 1741 ft-lbs (2260 Joules), resulting in a per thickness energy absorbing capacity of 243.2 ft-lbs/in (129.8 J/cm). Compared to Aramid ECLT, the average energy absorption capacity of the entire panel was 2067 ft-lbs (2803 Joules), leaving 401 ft-lbs (543 Joules) absorbed by the aramid layer when subtracting out the baseline CLT. The per thickness energy absorption capacity of the aramid layer when sandwiched between plies of CLT was 714 ft-lbs/in (381 J/cm), almost three times that of CLT. Although the aramid epoxy plate was adhered to the wood like the mild and hard steel enhancing layers, there was no physical evidence of delamination or cracking at the aramid wood interface (Fig. 8).

6.1.4. UHMWPE (Type 10)

One specimen of ECLT enhanced with an ultra-high molecular weight polyethylene (UHMWPE) panel was subjected to five shots with a target striking velocity of 2500 ft/s (762 m/s), resulting in an average penetration depth of 2.35-inches (6.0 cm). The projectiles penetrated through the front CLT section, but were stopped entirely by the front of the UHMWPE panel (Fig. 9). After the second shot, a small crack aligned with that projectile's entry hole, and developed on the side of the front 2-ply CLT section, suggesting that the panel's energy dissipation caused internal stresses in the CLT sections through the panel's mechanical connections [3]. Alternatively, the crack could have simply propagated from the projectile's entry hole along a flaw or grain line toward the edge of the specimen.

After the initial five shots were completed at the target striking velocity, the specimen was subjected to three additional shots at higher striking velocities to determine this ECLT configuration's limiting striking velocity. One projectile with a striking velocity of 4169 ft/s (1271 m/s) resulted in complete perforation of the ECLT specimen. The projectile's residual velocity upon exit was 560 ft/s (171 m/s). For all three additional shots, the magnitude of internal strains within the enhancing layer caused radial and tangential cracking of the wood plies on both sides of the panel. Similar to the mild steel plate configuration, bulging of the UHMWPE panel occurred on its front and back faces, causing indentations in the rear 3-ply CLT section beyond the enhancing layer. In general, the specimen withstood high velocities with minimal

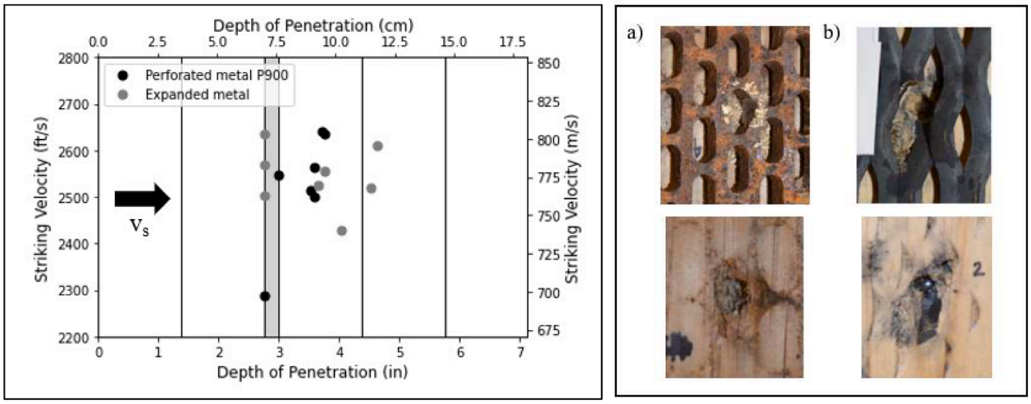

Fig. 5. Impact velocity versus penetration depth for perforated and expanded metal ECLT configurations (left) Widening of perforated metal gap (a) Fracturing of expanded metal captured in wood ply (b) (right).

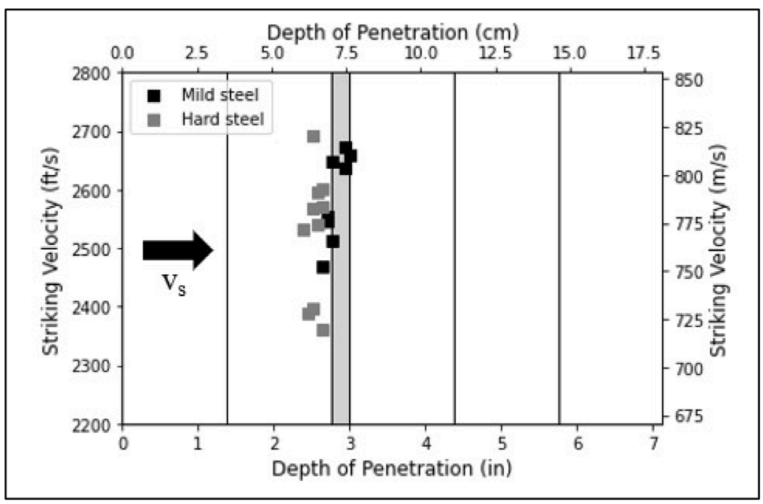

Fig. 6. Impact velocity versus penetration depth for mild and hard steel SYP ECLT configurations.

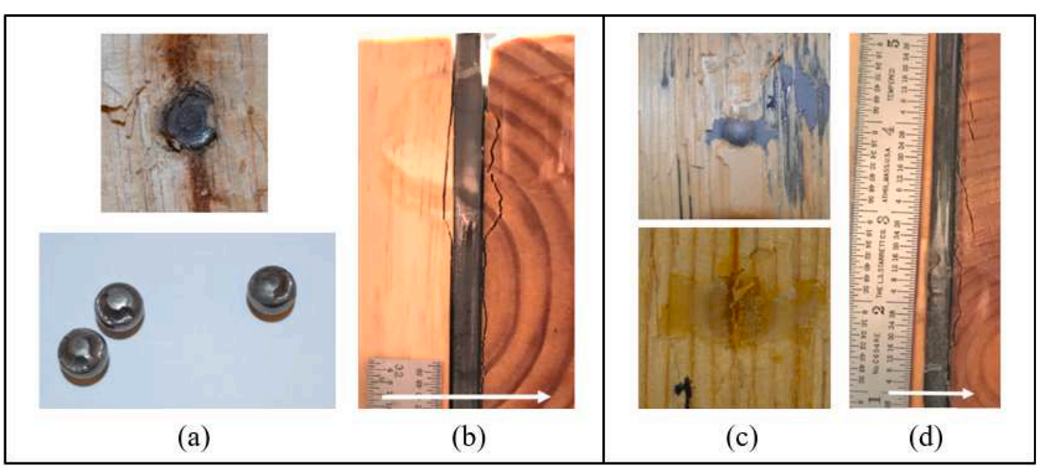

Fig. 7. (a) Plugging failure of hard steel plate embeds projectile sized plug into 3-ply face (b) Wood fracture observed after test shots at wood-hard steel interface (c) Bulge formed in mild steel and indentation in 3-ply CLT affixed behind steel (d) Evidence of wood fracturing at wood-mild steel interface.

impact to the CLT.

Using the striking and residual velocity from the perforated shot, the total energy absorbed by the panel was 4875 ft-lbs (6610 Joules). Subtracting the baseline CLT panel leaves 3209 ft-lbs (4351 Joules) absorbed by the UHMWPE enhancing layer which results in a per thickness energy absorption of 3209 ft-lb/in (1713 J/cm), over 13 times that of CLT. The high impact strength of UHMWPE was clear with testing, as the specimen withstood high velocities with minimal impact to the wood plies. The UHMWPE panel may have similar results on its own due to its specific design for ballistic resistance, but the lack of overall strength

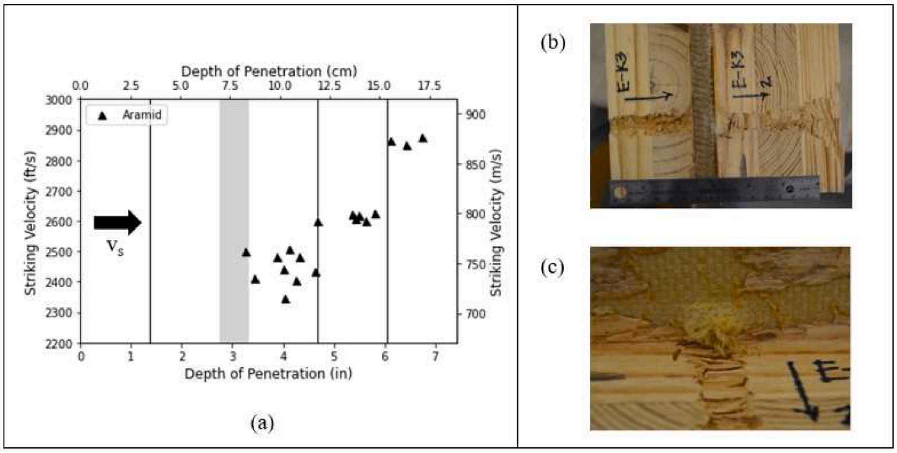

Fig. 8. (a) Impact velocity versus penetration depth for aramid SYP ECLT (b) Projectile path (c) Fracture of aramid fibers.

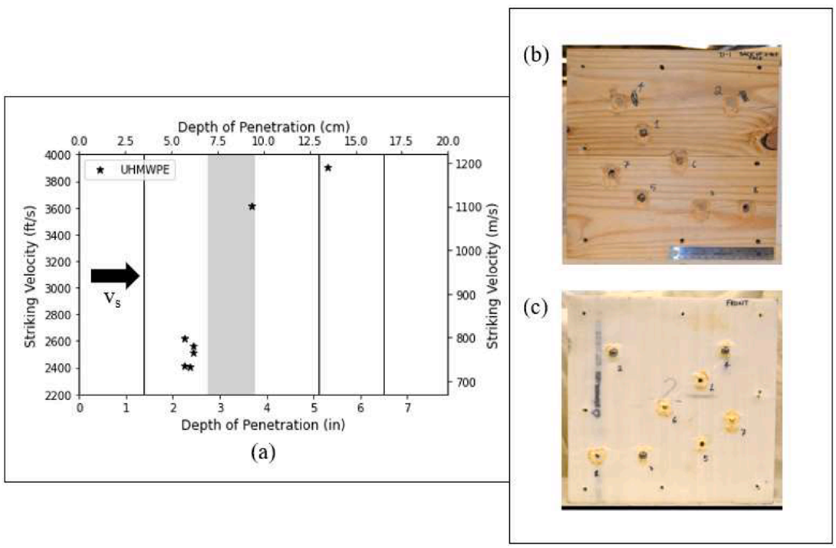

Fig. 9. (a) Impact velocity versus penetration depth for UHMWPE SYP ECLT configurations (b) Back of front 2-ply CLT (c) Front of UHMWPE panel.

and stiffness limits its use as a stand-alone structural panel. Utilizing UHMWPE within a CLT layup results in both enhanced force protection capacities and structural rigidity needed for wall systems.

6.1.5. E-glass

Two configurations of fiberglass enhanced CLT were tested with the same amount of fiberglass dispersed differently within the CLT layup, mainly as an initial study to assess if the distribution of enhancing material impacted ballistic resistance. The first configuration had one layer of consolidated fiberglass between the second and third ply, and the second configuration had four layers of fiberglass, one between each ply.

6.1.5.1. Consolidated 4-ply fiberglass (Type 11). Two specimens with consolidated single layers of fiberglass were tested with a target striking

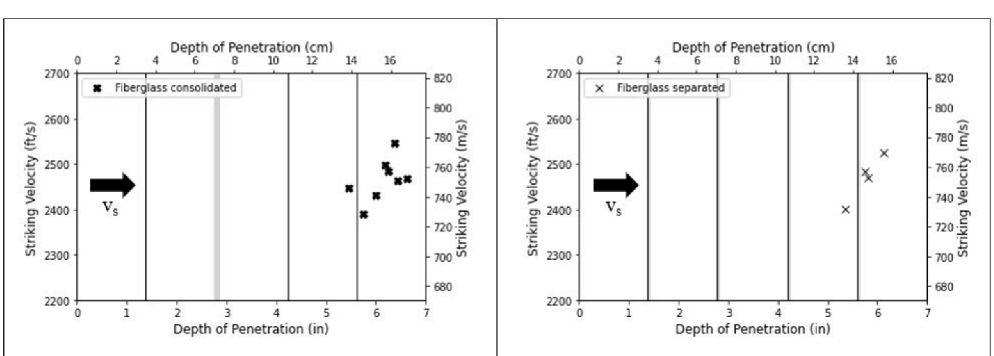

Fig. 10. Impact velocity versus penetration depth for consolidated fiberglass SYP ECLT (left) and separated fiberglass SYP ECLT (right).

velocity of 2500 ft/s (762 m/s), resulting in eight partial and two complete penetrations. The average penetration depth for the partially penetrated shots were 6.13-inches (15.57 cm), indicating penetration through the front CLT section, through the enhancing layer, and well into the rear CLT section. The residual velocities for the two complete penetrations were 301 ft/s (92 m/s) and 327 ft/s (100 m/s), and were characterized by wood petaling on the rear face of the specimen (the failure behavior also observed with typical CLT), and stretch and brittle fracture of the enhancing layer (Fig. 10).

6.1.5.2. Separated 4-ply fiberglass (Type 12). Similarly, two specimens with four separated layers of fiberglass were tested, resulting in four partial and eight complete penetrations. The average penetration depth for shots that partially penetrated was 5.76 inches (14.6 cm), and like the consolidated results, penetrated well into the back of the CLT panel. As the projectile slowed and reached the back face of the ECLT panel, the failure mechanisms of the fiberglass transitioned from brittle rupture to visible stretching, seen in Fig. 11.

The average residual velocity for shots that fully penetrated was 502 ft/s (153 m/s), and like the consolidated shots was characterized by wood petaling on the rear face of the panel. However, the damaged area was more localized with cratered spalling, potentially due to the higher exit velocities and free surface reflective wave effects. Fig. 11 plots striking versus residual velocity for the two configurations of fiberglass enhanced CLT as well as the unenhanced base panel. In the same range of striking velocities, more shots completely perforated when the fiberglass was distributed between each ply, and the average energy absorption of the consolidated fiberglass ECLT was nearly 73.8 ft-lb$_f$ (100 Joules) higher than the separated ECLT. The difference in overall performance suggests that the configuration of fiberglass fabric layers could be a significant factor for ballistic resistance, but this must be confirmed with more testing. Compared to a standard 5-ply CLT panel, which suffered complete penetration with every shot, residual velocities were significantly decreased with the addition of relatively thin layers of fiberglass.

6.2. SPF-S

The current database of ballistic CLT partial and full penetration experimental results mainly utilized 0.50-inch (1.27 cm) steel sphere or 0.50-inch (1.27 cm) fracture simulating projectiles (FSP) with the 0.50-inch (1.27 cm) sphere experimental data published in the literature [2]. However, contemporary projectiles are ogive shaped with different penetration mechanisms than spherical projectiles.

The following program assessed the performance of SPF-S ECLT under ogive shaped NATO threats within a range of typical muzzle velocities. While the experimental data is limited, the goal of the program was to assess the feasibility of integrating ECLT with comparable thicknesses to historically used materials while withstanding real NATO threats defined in DOS standards. Based off the 0.50-inch (1.27 cm) sphere ECLT results and from an economical point of view, steel enhancing layers were utilized. Low-carbon steel plates of 0.50-inch (1.27 cm) thickness have proven adequate in stopping the NATO test ammunition used [8], and therefore acted as the upper limit of enhancing material integrated in the SPF-S ECLT layups.

Because three different projectiles were utilized, the kinetic striking energy was plotted against depth of penetration in place of striking velocity because although the muzzle velocity for the M80 projectile was lower than the M193 and M855 projectiles, the mass was nearly three times as large. To better capture the threat impact, kinetic striking energies of the projectiles were used for comparison, and therefore it was assumed the projectile did not fracture or lose mass during penetration based on residual velocity camera footage and post testing deconstruction of the panels (Fig. 12).

6.2.1. Mild steel

CLT panels enhanced with two layers of thin (Type 5) and thick (Type 6) mild steel plates were tested with the projectiles and target striking velocities located in Table 2. The average penetration depth for each projectile type (M80, M193, M855) was 8.42 in (21.38 cm), 6.30 in (16 cm), and 7.78 in (19.76 cm), respectively for the Type 5 panel with two layers of thin mild steel plate reinforcement. This indicates that all projectiles penetrated well beyond the first layer of reinforcement, and the M80 round (largest striking kinetic energy) was ultimately stopped by the second layer or reinforcement. The average penetration depth for each projectile type was 6.16 in (15.66 cm), 4.39 in (11.14 cm), and 7.32 in (18.59 cm), respectively for the Type 6 panel with two layers of thick mild steel plate reinforcement. This indicates that all projectiles completely penetrated the first layer of steel reinforcement but were slowed enough to stop in the middle CLT plies before reaching the second layer of reinforcement. There were no complete perforations with either configuration, and a graphical representation of the penetration distributions can be found in Fig. 12.

6.2.2. Steel mesh

CLT panels enhanced with four layers of fine (Type 7) and two layers of coarse (Type 8) steel mesh, equaling the same amount of total enhancing material within the two types were tested with the projectiles and target striking velocities located in Table 2. For the Type 7 configuration, the average penetration depths for the M193 and M855 projectiles were 5.05 in (12.82 cm) and 5.90 in (14.97 cm), respectively, and the M193 projectiles were completely stopped before the third fine layer of steel mesh. Two out of three M80 shots completely perforated, with the only embedded shot stopped by the fourth and final layer of steel mesh. For the Type 8 configuration with two layers of coarse steel mesh, the average penetration depth for each projectile type was 8.65 in (21.97 cm), 6.05 in (15.36 cm), and 6.65 in (16.90 cm) respectively. All projectiles perforated the first layer of steel mesh with the M80

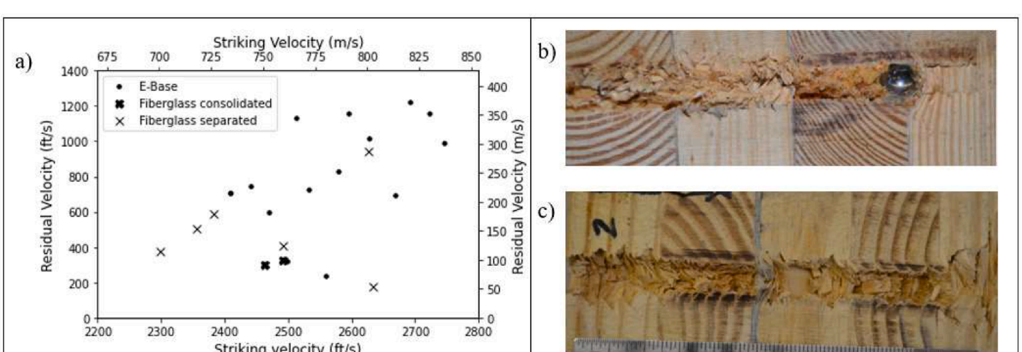

Fig. 11. (a) Impact velocity vs residual velocity for fiberglass SYP ECLT (b) Projectile stopped within separated fiberglass SYP ECLT (c) Projectile path through consolidated fiberglass SYP ECLT.

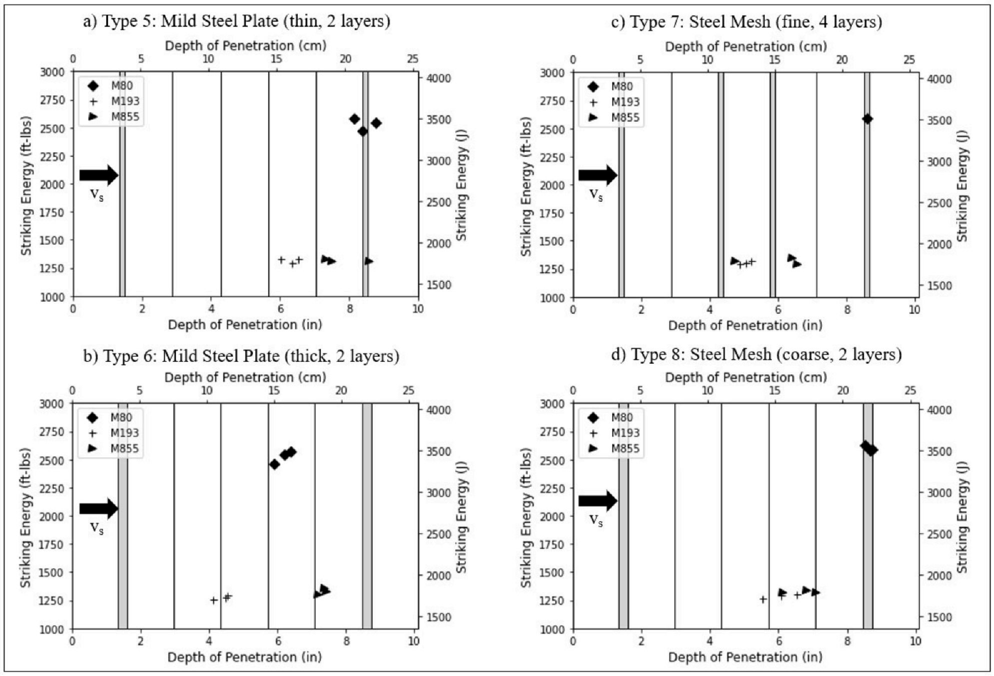

Fig. 12. Impact kinetic energy vs penetration depth for SPF-S ECLT with (a) two layers of thin mild steel reinforcement (b) two layers of thick mild steel reinforcement (c) four layers of fine steel mesh (d) two layers of coarse steel mesh.

projectiles ultimately stopped by the second layer steel mesh at the back of the specimen and the M193 and M855 projectiles were slowed enough by the first layer of steel mesh to stop in the wood laminate.

A similar amount of steel mesh enhancement, separated within the layup instead of consolidated in fewer layers yielded a shallower penetration for the M193 and M855 projectiles, indicating a better overall ballistic performance of the panel. However, the M80 projectile perforated two out of three shots with four thin layers compared to no perforations in the two coarse layers. This shows that the distribution of enhancing material within a layup impacts ballistic performance, depending on projectile type, striking velocity, and enhancing material choice.

7. Cost benefit analysis framework

The composite nature of ECLT allows for easy addition and modification of layup layers while designing a panel. Deciding what materials and thicknesses form a panel could be based on numerous factors, and requires a cost to benefit analysis to insure an optimized design for any given application. In conducting a cost to benefit analysis, it is imperative to define the benefit. Many contributing factors could be used to assess the benefit, such as ease of production and constructability, ballistic resistance, weight, etc. The list of potential “benefits” is extensive, so rather than calculate a simplified benefit cost ratio with arbitrary benefit metrics, an analysis approach will be discussed as well as the range of applicability within individual benefit criteria.

Like any optimization problem, relevant variables must be defined and weighted by importance. The same structure is proposed here where ECLT configurations could first be ranked by material weight, cost, ballistic resistance, or any other relevant benefit criteria, and weighted by importance to choose the optimal design. With the ability to change cost benefit criteria and normalize by rankings, situational decision making (extremely prevalent in force protection applications) becomes simplified and efficient. However, this decision-making structure is limited by available data as well as potential subjectively of some rankings. As an example, an examination of material weight for the current study as a benefit criterion will be discussed in the following section.

7.1. Weight analysis

A challenge with adding armor for improved force protection is optimizing overall material weight and protection. Perforated metals work towards this aim by integrating designed void spaces to reduce the actual amount of steel while keeping the general resistance level of the metal plate. New technologies in fiber-based composite laminates also provide new lightweight options. Panel weight is typically a lower priority for fixed, permanent building installations than for rapidly deployable modular structures. Given the cost benefit structure presented, the weight assigned to panel weight as a variable would drastically differ given these two applications.

7.1.1. Areal density

There is a finite amount of surface area on a vehicle, aircraft, structure or person to protect, and the areal density describes the weight over that area. Manufacturers cite areal density as a material characteristic of composite ballistic panels, which often gives an indication of the energy absorbing capacity of the material. Table 3 provides the areal density and weight of each enhancing layer material used in the SYP ECLT specimens.

Mass efficiency is used to measure effectiveness of armor materials. It is calculated relative to the areal density of rolled homogeneous armor (RHA), the steel plate typically used on tanks. The areal density of the RHA steel plate of the designated thickness required to stop a specified threat is divided by the areal density of the armor material under consideration. The higher the mass effectiveness, the lighter the weight of the armor for the same threat.

Presented is the full weight and areal density breakdown for the enhancing materials used in the SYP ECLT required to inform the ranking of heaviest to lightest for this benefit criterion. Although the fiber composites are advantageous to the metals by weight, other factors such as environmental exposure or permanency of a structure would impact the benefit cost analysis. This weight and areal density data mainly act as an example of what data would be imported into the

Table 3
Areal Density of Enhancing Materials.

Enhancing Layer		Thickness in. (cm)	Weight of layer lb. (kg)	Mass density lb/in^3	Areal density of enhancing layer(s) lb/in^2 (kg/m^2)
Type 1	P900 Perforated Steel Plate	0.50 (1.27)	10.00 (4.54)	719.96	20.00 (97.64)
Type 2	Expanded Metal Plate	0.50 (1.27)	6.23 (2.82)	448.21	12.45 (60.79)
Type 3	Aramid Epoxy Panel	0.56 (1.42)	3.56 (1.61)	288.31	6.33 (30.89)
Type 4	Mild Steel Plate (1 layer)	0.25 (0.63)	10.26 (4.66)	369.52	41.06 (200.46)
Type 9	High-Hard Steel Plate	0.25 (0.63)	9.74 (4.42)	350.62	38.96 (190.21)
Type 10	Ultra-High Molecular Weight Polyethylene (UHMWPE)	1.00 (2.54)	5.12 (2.32)	737.79	5.12 (25.02)
Type 11	Fiberglass Fabric (4-ply consolidated)	0.12 (0.31)	0.51 (0.23)	8.79	4.24 (20.70)
Type 12	Fiberglass Fabric (4-ply separated)	0.12 (0.31)	0.13 (0.0577)	8.79	4.24 (20.70)

benefit cost optimization structure. Ultimately this structure puts control in the hands of decision makers rather than defining a preset benefit-cost framework. This allows adaptability and updating abilities with additional distribution of relevant data.

8. Analytical model discussion

To accompany the experimental results presented, a multi-material wood analytical model was developed that can be used as an initial framework for ECLT. The general methodology is presented in Fig. 13 for a mild steel enhanced SYP CLT panel (as an example). In this approach, there are n layers of material. Each layer is numbered $i = 1$ *to* n, and the penetration through each layer is governed by the corresponding penetration equation for that material. The striking velocity of each layer is equal to the residual velocity of the layer before ($i - 1$ layer), and the layer behaviors are aggregated until either the velocity equals zero (i.e., the projectile stops in that layer) or the projectile passes through the n^{th} layer and the residual velocity is predicted. The goal of this framework approach is to use existing data and predictive ballistic design models for individual material layers to incrementally aggregate performance through the depth of an ECLT panel.

Previously, THOR physics based empirically fit partial and full penetration equations for wood were developed and calibrated for CLT using SPF-S and SYP experimental results [2], and will be used for the wood layers (Eq. (1)). The equation includes depth of penetration, DOP, striking velocity of the projectile, v_s, as well as density, ρ, and hardness values, H of the wood species used. Using this calibrated equation, the residual velocity, v_r, is zero when the penetration depth is equal to or less than the thickness of CLT, t, considered. A new variable, v_{per}, is defined as the perforation velocity or maximum striking velocity that does not result in perforation (Eq. (2)). The residual velocity of a CLT layer can therefore be computed as the difference between striking velocity and perforation velocity [2]. However, through experimental investigation it has been found that the projectile has less resistance as it reached the back face of the CLT, so the model would underpredict residual velocities. Therefore, a reduction factor, R, was added as a calibration factor. Eq. (3) is the complete model formulation for CLT layers in the aggregated model. Note that in these equations, the projectile is constant with *f, g, a, b,* and *R* as calibration constants.

$$DOP = C_1\left(\frac{v^f}{10^g \rho^a H^b}\right) \tag{1}$$

$$v_{per} = \left(\frac{\mathrm{t}}{C_1}\left(10^g \rho^a H^b\right)\right)^{(1/f)} \tag{2}$$

$$v_r = v_s - Rv_{per} \tag{3}$$

The enhancing materials used in this study are independently highly ballistic resistant and are currently integrated in force protection applications such as body or vehicle armor. Although CLT and wood composites have more recently been studied under high rate loading events, the enhancing materials are backed by numerous research and experiments. This proposed framework leverages past research and model development, which aims to limit the amount of new experiments needed to refine the model.

Using the Type 4 mild steel plate ECLT experimental results, validity of the analytical model was assessed. For experiments with a target striking velocity of 2500 ft/s (762 m/s), all shots were embedded in the steel layer. For the steel layer, the UFC equation was utilized (Eq. (4)) with variables thickness of steel plate, t, impact velocity, v, diameter of

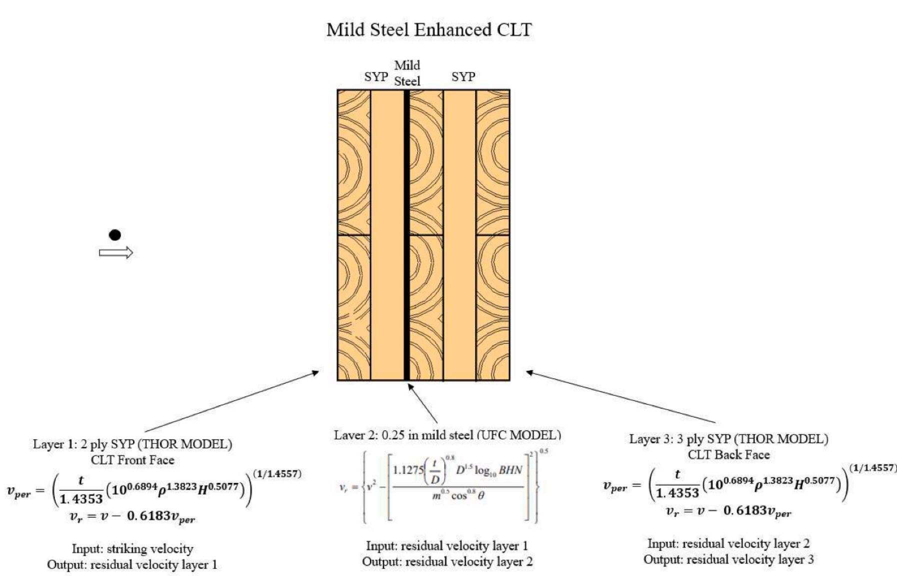

Fig. 13. Multi-material model framework schematic.

projectile, D, mass of projectile, m, Brinnel Hardness Number, BHN, and residual velocity, v_r.

$$v_r = \left\{ v^2 - \left[\frac{1.1275\left(\frac{t}{D}\right)^{0.8} D^{1.5} log_{10} BHN}{m^{0.5}} \right]^2 \right\}^{0.5} \tag{4}$$

Using the analytical approach, the depth of penetration results agrees with the experiment where the projectile does not continue past the steel layer, but due to the ductile plugging failure mechanisms of steel extended slightly into the next SYP CLT layer (Fig. 7c). This example evaluation utilized THOR CLT and UFC steel equations, but others could be substituted in as models get refined with higher fidelity.

Although this experimental study was focused on non-wood enhancing layers, this approach can be applied to solely layered wood composites like CLT. To evaluate the validity of this framework, say two SPF-S CLT panels are placed together, one a two ply and the other a three ply with no adhesive between the two- and three-ply panels. If fully perforated, the model predicts a slightly lower residual velocity compared to a five-ply SPF-S CLT with adhesive between all layers. This identifies gaps in the framework, where residual velocity ballistic equations are used for all perforated layers, confined or unconfined, and the effects of the interface between layers is not considered.

Although out of scope for this study, the supplementation of interface mechanics and confinement effects to the current multi-layer analytical model approach would refine predicted depth of penetration and residual velocity results, and is a key area of future study as the increase of mass timber composites are integrated into force protection applications.

9. Conclusions

The layered nature of CLT allows its composition to be modified for design requirements, such as ballistic resistance. Various ECLT specimens were fabricated and tested for ballistic resistance using Multiple species of wood, enhancing materials, and projectile types.

ECLT specimens with solid steel plates exhibited greater ballistic resistance than standard CLT. Those with perforated metal plates performed comparably to those with solid steel plates, but were less heavy. Specimens with fiber-based ballistic panels also increased the ballistic resistance of the panel and were significantly lighter than the product with metal plates. The fiber-based materials also bonded well to the CLT with an epoxy mixture with four very thin fiberglass fabric layers notably improving the specimen's ballistic resistance, although some perforating shots were observed. Finally, this research proved that steel reinforced ECLT can prevent complete perforation of NATO ogive nose projectiles at realistic striking velocities.

Frameworks for both a cost-benefit assessment and multi-material analytical model were developed and discussed as part of this proof-of-concept study to lay the foundation for future research requirements. Based on the results of these experiments, it is evident that different specimens should be produced and tested to optimize the key factors of an ECLT panel configuration, such as: type of enhancing layer, location of enhancing layer along CLT panel depth, weight of enhancing material. Additional research in this area would greatly improve specialized uses for CLT, particularly for temporary military structures.

CRediT authorship contribution statement

Juliet Swinea: Methodology, Software, Formal analysis, Investigation, Writing – original draft, Writing – review & editing, Visualization. **Kathryn Sanborn:** Conceptualization, Software, Investigation. **Mark Weaver:** Software, Formal analysis, Writing – original draft, Project administration, Funding acquisition. **Marco Lo Ricco:** Resources, Writing – original draft. **C.Adam Senalik:** Resources, Writing – original draft. **Lauren K. Stewart:** Conceptualization, Methodology, Formal analysis, Writing – original draft, Writing – review & editing, Project administration, Supervision, Funding acquisition.

Declaration of competing interest

The authors declare that they have no known competing financial interests or personal relationships that could have appeared to influence the work reported in this paper.

Data availability

The data is included as supplemental materials.

Acknowledgements

This work was partially supported by the United States Forest Service (USFS) through the Wood Innovations Grant under USFS Domestic Grant 17-DG-11083150–008. Any opinions, findings, and conclusions or recommendations expressed in this material are those of the authors and do not necessarily reflect the views of the United States Forest Service. The authors would like to acknowledge the support of Dr Richard McGee, Mr Don Little, Dr Bill Heard, and Dr Jesse Sherburn at the US Engineer Research and Development Center, the support of Mr Charles Randow and the US Army Research Lab, and the support of Dr Christopher Conley and the United States Military Academy for their assistance with the experimental program.

This work was also partially funded by the USDA, Forest Service, Wood Innovations Grant No. 2019-DG-11052021–226 and was made possible through contributing funds provided by the Softwood Lumber Board. SmartLam North America manufactured the SPF-S ECLT panels. H.P. White Laboratory performed the ballistic resistance tests on the SPF-S ECLT panels.

Supplementary materials

Supplementary material associated with this article can be found, in the online version, at doi:10.1016/j.ijimpeng.2024.104931.

References

[1] Weaver M, et al. Development of a cost-effective clt panel capable of resisting dos/dod design basis threats. Glendale, CA: Karagozian & Case, Inc.; 2020.
[2] Sanborn K, Gentry TR, Koch Z, Valkenburg A, Conley C, Stewart LK. Ballistic performance of cross-laminated timber (CLT). Int J Impact Eng 2019;128:11–23.
[3] SANBORN KATHRYN, et al. Ballistic Performance of Enhanced Cross-Laminated Timber (ECLT). WIT Trans. Built Environ. 2018.
[4] Flores NR, Gentry R, Stewart LK. Behavior and damage characterization of impulsively loaded cross-laminated timber panels. Appl. Sci. 2022;12(23):12076.
[5] PDC-TR 18-02, "Analysis Guidance for Cross-Laminated Timber Construction Exposed to Airblast Loading, "U.S. Army Corps of Engineers Protective Design Center, Omaha District, September 2018.
[6] Swinea Juliet, et al. Effect of thermal modification on the ballistic performance of coastal Western Hemlock cross-laminated timber (CLT). Int J Impact Eng 2023; 182:104769.
[7] Weaver MK, Newberry C, O'Laughlin C, Podesto L. Results from blast tests of full scale cross-laminated timber structures. Karagozian & Case, Inc.; 2017. TR-17-17.1September.
[8] Karacabeyli E, Douglas B. CLT handbook (Cross-Laminated timber). U.S. Edition; 2013.
[9] Sanborn K. Exploring Cross-Laminated Timber Use for Temporary Military Structures: Ballistic Considerations. PhD thesis. Atlanta, GA: Georgia Institute of Technology; 2018.
[10] Lowak MJ. Static and dynamic testing of cross-laminated timber panels. San Antonio, TX: Baker Engineering and Risk Consultants, Inc.; 2015. 29 June.
[11] Lowak MJ. Additional static and dynamic testing of cross-laminated timber panels. San Antonio, TX: Baker Engineering and Risk Consultants, Inc.; 2016. 10 February.
[12] Poulin M, Viau C, Lacroix D, Doudak G. Experimental and Analytical Investigation of Cross-Laminated Timber Panels Subjected to Out-of-Plane Blast Loads. J Struct Eng. 2018;144(2).
[13] Viau C, Doudak G. Behaviour and modelling of cross-laminated timber panels with boundary connections subjected to blast loads. Eng Struct 2019;197.

[14] Lopez-Molina A, Doudak G. Retrofit techniques for Cross-Laminated Timber (CLT) elements subjected to blast loads. Eng Struct 2019;197. 15 October.

[15] Bhat Aayush, et al. Advancement in fiber reinforced polymer, metal alloys, and multi-layered systems for Ballistic Applications – A Review. J Mater Res Technol 2021;15.

[16] Odesanya Kazeem Olabisi, et al. Natural fibre-reinforced composite for the ballistic applications: a Review. J Polym Environ 2021;29(12).

[17] Ranaweera Prabhani, et al. Ballistic performance of mulit-metal systems. Int J Protective Struct 2020;11(3).

[18] U.S. Department of Defense. Unified facilities criteria, design to resist direct fire weapons effects (UFC 4-023-07). Washington D.C.: U.S. Department of Defense; 2008. with 2017 update.

[19] Gupta NK, Madha V. An experimental study of normal and oblique impact of hard-core projectile on single and layered plates. Int J Impact Eng 1997;19:395–414.

[20] Performance Specification: Perforated Homogeneous Steel Armor, eds DOT Army, Army Research Laboratory, Aberdeen Proving Ground, MD, Weapons and Materials Research Directorate, Materials Applications Branch, and Specifications and Standards Office, 2007.

[21] Wang Caizheng, et al. On the Mechanical Behaviour of Steel Wire Mesh Subjected to Low-Velocity Impact. Thin-Walled Struct 2021;159:107281. https://doi.org/10.1016/j.tws.2020.107281.

[22] Kılıç Namık, Ekici Bülent. Ballistic resistance of high hardness armor steels against 7.62mm armor piercing ammunition. Mater Des 2013;44:35–48.

[23] van Dingenen JLJ. High performance dyneema fibres in composites. Mater Des 1989;10:101–4.

[24] Aicher S, Hirsch M, Christian Z. Hybrid cross-laminated timber plates with beech wood cross-layers. Constr Build Mater, 124 2016:1007–18.

[25] Davids WG, et al. Structural performance of hybrid SPFs-LSL cross-laminated timber panels. Constr Build Mater 2017;149:156–63.

[26] Wang Z, et al. Planar shear and bending properties of hybrid CLT fabricated with lumber and LVL. Constr Build Mater 2017;151:172–7.

[27] Wang Z, Gong M, Chuim YH. Mechanical properties of laminated strand lumber and hybrid cross-laminated timber. Constr Build Mater 2015;101:622–7.

[28] The Engineered Wood Association. American national standard: standard for performance-rate cross-laminated timber ansi/apa prg 320-2012. Tacoma, WA: APA; 2012.

[29] SD-STD-01.01, Rev. G. Forced entry and ballistic resistance of structural systems (Certification standard). Washington, D.C.: U.S. Department of State, Bureau of Diplomatic Security, Office of Physical Security Programs, Physical Security Division; 1993. 30 April.